Eur Respir J, 1996, 9, 2461–2467
DOI: 10.1183/09031936.96.09122461
Printed in UK - all rights reserved

European Respiratory Journal
ISSN 0903 - 1936

Effect of frusemide on Cl⁻channel in

G. Meyer*, S. Doppierio*, P. Vallin*, L. Daffonchio**

Effect of frusemide on Cl⁻channel in rat peritoneal mast cells. G. Meyer, S. Doppierio, P. Vallin, L. Daffonchio. ©ERS Journals Ltd 1996.

ABSTRACT: Frusemide can be used as an antiasthma drug and appears to inhibit the release (conditioned by activation of Cl^- channels) of mast cell proinflammatory mediators. We studied the cause of the effects of frusemide, checking its action on Cl^- channels.

The patch-clamp technique was used to study single-channel currents, and differences in electrical potential of the cellular membrane of rat peritoneal mast cells were measured.

In inside-out configuration, outwardly-rectifying Cl^- channels were identified whose conductance was 2.4/1.7 pS at positive and negative voltages. In cell-attached configuration, the open probability (P_o) of the channel increased with depolarization or with the presence of cyclic adenosine monophosphate (cAMP) in the incubation medium. P_o increased with a rise of cytoplasmic free calcium concentration [Ca^{2+}] and was inhibited by 5-nitro-2-(3-phenylpropylamino)-benzoate (NPPB) and by 4-4'-diisothiocyanatoostilbene-2-2'-disulphonic acid (DIDS). These channels seem to be the main cause of mast cell Cl^- conductance. Frusemide (10^{-5} and 10^{-3} M) did not affect Cl^- channel activity when using excised patches. In cell-attached configuration experiments, the presence of frusemide (from 10^{-8} to 10^{-3} M) in the cell incubation medium, increasingly reduced P_o (median inhibitory concentration (IC_{50}) $=4.3\times10^{-7}$ M). In similar conditions, bumetanide also inhibited P_o ($IC_{50}=5.7\times10^{-8}$ M).

The results of this study suggest that frusemide can inhibit mast cell Cl^- channels only *via* an indirect mechanism, which probably involves an inhibition of a Na^+-K^+-$2Cl^-$ symport.

Eur Respir J., 1996, 9, 2461–2467.

*Dipartimento di Fisiologia e Biochimica Generali, Sezione di Fisiologia Generale, Università degli Studi di Milano, and **Dompè Spa, Milano, Italy.

Correspondence: G. Meyer
Dipartimento di Fisiologia e Biochimica Generali
Via Celoria 26
20133 Milan
Italy

Keywords: Bumetanide
Cl^- channels
frusemide
mast cells

Received: October 12 1995
Accepted after revision August 5 1996

This research was supported by the Minestero dell'Università e della Ricera Scientifica e Tecnologica, Rome, Italy.

Mast cells play a fundamental role in the pathogenesis of asthma. Exposure to allergens can lead to the release, by mast cells, of proinflammatory mediators able to interact with airway epithelium, submucosal glands, the capillary wall and other inflammatory cells [1]. The rel-ease of these mediators involves the activation of a G protein and, through inositol 1,4,5 triphosphate, the rise of Ca^{2+} intracellular levels. The entry of Ca^{2+} into the cells is encouraged by the activation of specific Ca^{2+} channels and of aspecific cationic channels, but also by the hyperpolarization of the membrane caused by the increase of Cl^- conductance [2, 3]. The importance of the variation of this Cl^- conductance, shown by patch-clamp experiments in whole-cell configuration [3, 4], but not by single-channel data, has yet to be completely established, and other possible roles have been suggested [4]. Inhibitors of Cl^- conductance, such as 4-4'-diisothiocyanatostilbene-2-2'-disulphonic acid (DIDS) [4] or 5-nitro-2-(3-phenylpropylamino)-benzoate (NPPB) [5] have been seen to inhibit the degranulation of mast cells or rat basophilic leukaemia (RBL) cells, respectively, even though the evaluation of mediator release can be complicated by the stilbene interaction with enzyme activity, whose release can be used as a secretion indicator [4].

Frusemide is a diuretic, used for many years now by clinics in the treatment of fluid retention, in heart failure and for the control of hypertension; and, recently, its use has been proposed in the treatment of asthma [6]. It has been noted that frusemide [6, 7] can prevent the bronchospasm induced in asthmatic subjects by different stimulants, an action that appears to involve different mechanisms, including inhibition of airway nerves, induction of prostaglandin release, and inhibition of the release of mediators by mast cells, eosinophils or macrophages. In relation to this, it has been seen that the exposure of sensitized animals to frusemide aerosol was associated with a marked reduction of the bronchoconstriction induced by specific antigen and of the levels of histamine plasma [8]. In addition, *in vitro* frusemide significantly reduced the immunological release of histamine by mast cells of ovalbumin sensitive rats [8]. Frusemide is a well-known inhibitor of the Na^+-K^+-$2Cl^-$ symport [9, 10], but in many cells also of Cl^- channel activity [11, 12]. We thus decided to characterize, through a patch-clamp study, single Cl^- channels present in mast-cells and to verify the action of frusemide and other specific inhibitors of Cl^- channels.

Materials and methods

Preparation of mast cells

Rat mast cells were obtained by means of a modification of a previously described method [13]. The animal was anaesthetized and decapitated, and 8 mL of an isolation solution (Solution A, see next section) was injected into the peritoneal cavity, obtaining a suspension containing mast cells. This suspension was centrifuged (Swing out rotor, Hermle 200.27) at 4°C for 1 min at 220×g. The pellet was resuspended in 2 mL of Solution B, and this was stratified in a test tube containing a 30/40% (w/v) Ficoll gradient. This suspension was centrifuged at 1,060×g for 10 min at 4°C, and the upper two-thirds of the liquid was discarded. Two successive washings were then performed (10 min, 4°C, at 2,260 and 1,770×g respectively). Finally, the pellet was resuspended in 1 mL of Solution B. Before the experiment, 200 µL of suspension was placed on a slide and then in a small Petri dish and cellular incubation medium was added. Patch-clamp experiments were performed at 22±1°C. Any possible contamination by other cells (toluidine blue method [14]) was negligible and vitality was over 80%.

Solutions

Solution A contained (mM): 145 NaCl, 6 KH_2PO_4, 0.4 Na_2HPO_4, 5.5 glucose and human serum albumin (HSA) 0.1% w/v (pH 6.0). Solution B contained (mM) 145 NaCl, 2.5 KCl, 1.2 $CaCl_2$, 1.3 KH_2PO_4, 2.6 Na_2HPO_4, 5.5 Glucose and HSA 0.1% w/v (pH 7.4). During the experiment the isolated cells were kept in a solution containing (mM): 140 NaCl, 5 KCl, 1 $MgCl_2$, 2 $CaCl_2$, 10 N-Tris-(hydroxymethyl)methyl-2-aminoethanesulphonic acid (TES)/NaOH (pH 7.4), 10 glucose. In some experiments this solution contained 8-bromoadenosine 3':5'-cyclic monophosphate (8-Br-cAMP).

The micropipette solution, used for experiments in cell-attached or in inside-out configuration, contained (mM): 145 N-methylglucamine-Cl, 10 TES/N-methylglucamine (pH 7.4), 3 ethylene glycolbis (β-aminoethylether)-N,N,N',N'-tetra-acetic acid (EGTA) and $CaCl_2$ to achieve a free calcium concentration $[Ca^{2+}]$ of 2×10^{-7} M.

The solution used on the cytoplasmic side in inside-out configuration experiments was similar to the micropipette filling solution and contained sufficient $CaCl_2$ [15, 16] to achieve a free $[Ca^{++}]$ of 2×10^{-7}, 10^{-6} or 10^{-4} M. In some cases 130 mM N-methylglucamine-gluconate and 15 mM N-methylglucamine-Cl or 145 mM KCl or 145 mM NaCl replaced N-methylglucamine-Cl. The function of cyclic adenosine monophosphate (cAMP) in the incubation medium was to activate Cl^- channels, avoiding the mast cell degranulation [3].

The microelectrode filling solution used for whole-cell configuration experiments contained (mM): 132 K-gluconate, 20 NaCl, 1 $MgCl_2$, 10 TES/KOH (pH 7.2), 0.2 EGTA, 0.5 adenosine triphosphate (ATP), 0.05 cAMP and 0.3 guanosine triphosphate (GTP). When the incubation medium was cAMP-free, the microelectrode solution did not contain cAMP either.

The microelectrode solution used for the perforated-patch technique contained (mM): 132 K-gluconate, 20 NaCl, 1 $MgCl_2$, 10 TES/KOH (pH 7.2), $CaCl_2$ and EGTA to achieve a free $[Ca^{2+}]$ of 2×10^{-7} M, nystatin (200 $\mu g\cdot mL^{-1}$) and Pluronic F-127 (0.05%).

Patch-clamp technique

The patch-clamp technique and data analysis were applied as reported previously [17]. For cell-attached (*i.e.* when the pipette is tightly sealed onto a cell to separate the patch area from the rest of the membrane [18]) and excised-patch experiments, microelectrodes with a resistance of 10^{-15} MΩ were used. Seals had a resistance in the range of 10–50 GΩ. The signals were filtered at 100–200 Hz with an eight-pole Bessel filter. The bath was grounded with an $Ag/AgCl_2$ electrode immersed in an agar bridge, with the ionic composition of the initial cellular incubation medium or with 1 M KCl (inside-out experiments, *i.e.* when the cytoplasmic face of the membrane was exposed to the bath solution [18]). Junction potentials were taken into account. When patches contained multiple channel openings, the open probability (P_o; the ratio of open time to total time of single channel recordings) was calculated as reported previously [17, 23]. Most of the data were obtained at positive voltages, because at high negative voltages the seals tended to be less stable. In cell-attached configuration experiments, potentials were expressed as overall potentials, considering both mean cellular membrane electrical potential difference, PD_{cm}, and holding potentials. In cell attached configurations the reversal potential was calculated on the basis of linear regression of points representing outward currents, since the currents observed for negative voltages appeared with very low frequencies and usually with amplitude values less than twice that of noise. Analyses were performed using a patch-clamp analysis program (PClamp 5.5, Axon Instruments Inc.). The gluconate permeability relative to Cl^- was calculated using the following equation:

$$Vr = \frac{RT}{F} \cdot \ln \frac{[Cl^-]_i + (P_{gluconate}/P_{Cl}\ [gluconate^-]_i}{[Cl^-]_o}$$

where Vr is the reversal potential, subscript i denotes bath and o pipette solution, and R, T and F are the molar gas constant, absolute temperature and Faraday constant, respectively.

The PD_{cm} was measured using whole-cell (*i.e.* the cytoplasmic side of the cell is in direct contact with the pipette solution [18]) configuration and current-clamp conditions (I=0) immediately after patch breaking. Nystatin perforated-patch technique (the antibiotic perforates the patch forming channels permeable to monovalent ion [18]) was also performed to measure PD_{cm}. The microelectrode for the whole-cell or nystatin perforated patch had a resistance of 2–3 MΩ.

Impalements using conventional or Cl^- selective microelectrodes

Conventional microelectrodes, and measurement setup, were similar to those described previously [19].

Microelectrodes were back-filled with 0.5 M KCl and resistance was 40–70 MΩ (tip diameter <0.2 µm). Microelectrodes were connected to a high input impedance electrometer (Kethley 617) and to a strip chart recorder (Linear 1200). Criteria for accepting a measurement of PD_{cm} were [20]: 1) an abrupt change of potential on entering a cell; 2) a constant value for at least 10 s; and 3) a rapid return of the potential to the original value on leaving the cell.

Cl^- selective single-barrelled microelectrodes were constructed with a Cl^- sensitive resin (Corning Cl^- Micro Exchanger 477913), and 154 mM KCl back-filled. They had a resistance of 1–4 GΩ. The method of construction, calibration and estimation of intracellular Cl^- activities ($a_{,iCl}$) was similar to that described previously for other selective microelectrodes [20, 21]. Potential difference due to a Cl^- activity change from 11.2 to 112.4 mM [22] was -53.9±0.4 mV (26 microelectrodes). The activity coefficient for Cl^- (the ratio between its activity and concentration) is 0.73 [24]. In this way it is possible to convert activity to concentration (and vice versa) allowing comparison of activities measured with selective microelectrodes and concentrations deduced from reversal potentials of I/V relationships.

Statistics

Experimental values are expressed as mean±SEM unless otherwise stated. In the text "n" is the number of animals. The data obtained from experiments of the same type, performed on cells from the same animal, have been averaged to obtain a single value. The Student's t-test was used (paired data where not specified) for the statistical analysis. A p-value of <0.05 was considered significant. Dose-response data were fitted to the Hill equation.

Results

Cl^- channel and its activation

In the absence of cAMP in the cellular incubation medium, the PD_{cm} measured in whole-cell configuration was -11.8±2.1 mV (n=5). To verify the reliability of these measurements, we performed impalements with conventional microelectrodes and measurements with nystatin perforated patch technique. The PD_{cm} values were -12.9±2.6 mV (n=4) and -10.1±2.7 mV (n=4), respectively. These values did not differ significantly from those determined in whole-cell configuration or from each other. Figure 1a shows recordings of currents passing through a single-channel obtained in cell-attached configuration (the microelectrode contained 145 mM N-methylglucamine-Cl, free cyclic adeosine monophosphate incubation medium). The appearance of these currents took place in about 50% of patches: in every case the P_o values were low (at -100 mV, P_o was 0.003± 0.001; n=10), but increased when changing to positive voltage (as suggested by fig. 1a; at 110 mV P_o was 0.082±0.004; n=10, p<0.01).

Figure 1b shows the current/voltage (I/V) relationship; the intercept with V axis was -62.9±4.1 mV (n=10). This value agrees with the behaviour of a Cl^- channel and with the $a_{,iCl}$ value determined in the absence of cAMP ($a_{,iCl}$=9.7±l.7 mM (n=4); the activity coefficient should be 0.73 [22]).

As a consequence of the addition of cAMP (250 µM) to the incubation medium, the PD_{cm} (whole-cell configuration) hyperpolarized to -37.9±2.7 mV (n=6). Using impalements or nystatin perforated-patch technique the values of PD_{cm} measured were not significantly different from those obtained with the previous method (-36.4 ±3.1 mV (n=4) and -40.9±3.6 mV (n=4), respectively). We observed an increase (at the tested voltages; p<0.05) in the P_o as shown in figure 2b. The I/V relationship (fig. 2c) showed a reversal potential of -41.9±3.4 mV (n=10), not significantly different from the measured PD_{cm} (in agreement with a PD_{cm} dominated by Cl^- conductance). This value of the inversion point does not differ from that forecast based on $a_{,iCl}$, 21.5±2.9 mM (n=4), determined with selective microelectrodes.

By using cAMP pretreated cells, changing to inside-out configuration (N-methylglucamine-Cl symmetrical solutions), we observed the tracings presented in figure 3a. Figure 3b shows the I/V relationship: on the basis of positive or negative currents, the reversal potential was

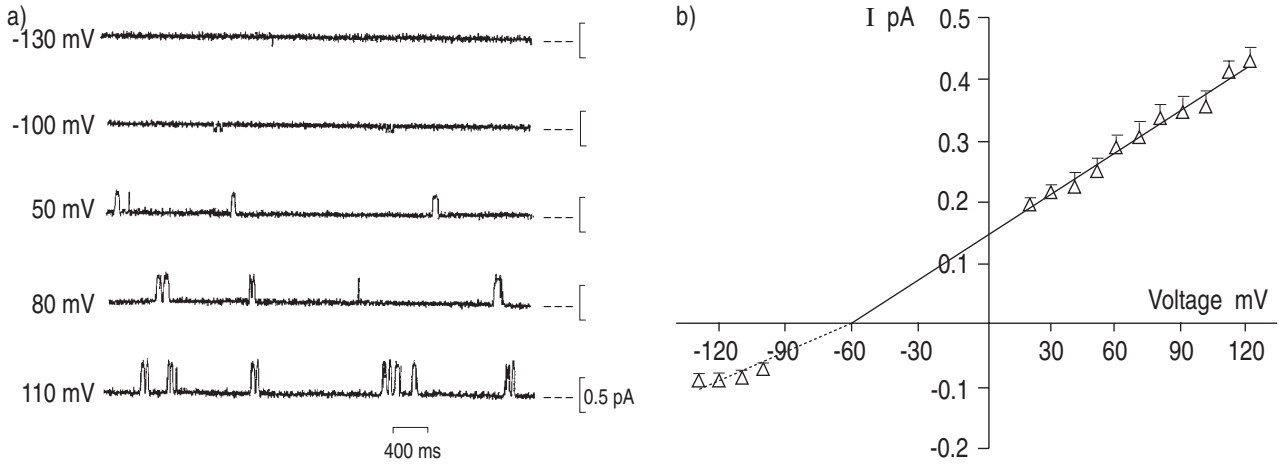

Fig. 1. – Single-channel currents (I) recorded, in cell-attached configuration, using a free cyclic adenosine monophosphate (cAMP) incubation medium (the microelectrode solution contained 145 mM N-methylglucamine-Cl). a) Tracings obtained at the voltages indicated. b) Single-channel current/voltage (I/V) relationship (the reversal potential was calculated on the basis of liner regression of points representing outward currents). Values are presented as arithmetic mean±SEM (n=10 animals).

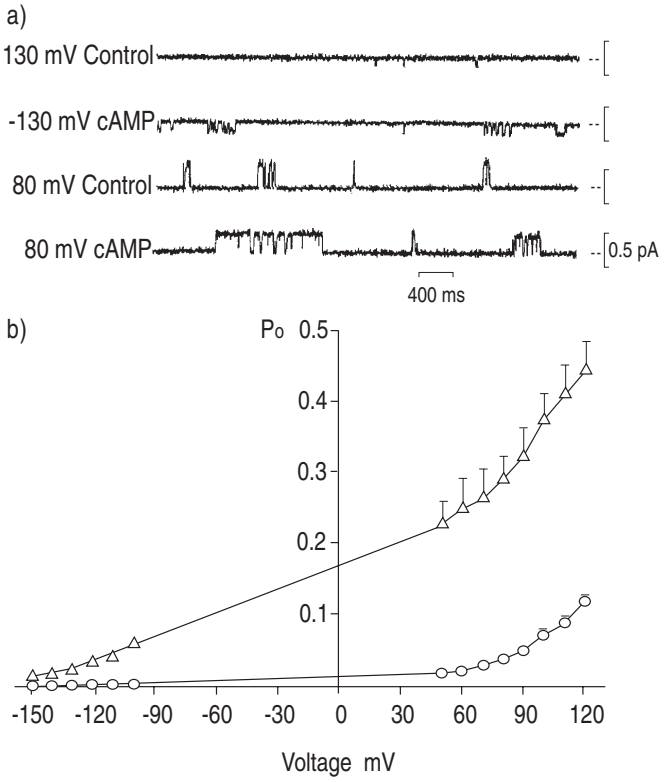

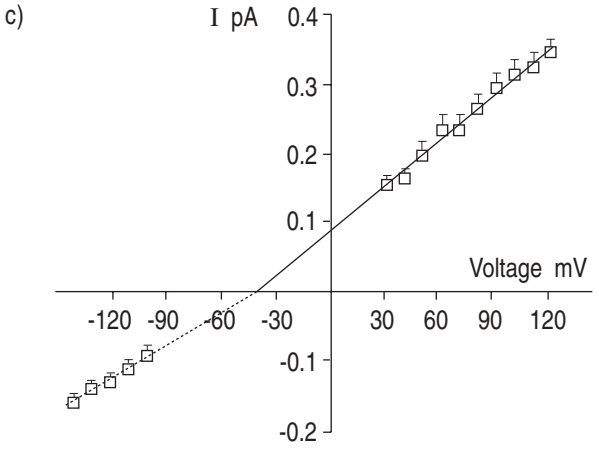

Fig. 2. – Open probability (Po) correlated to voltage in cell-attached patch in the absence or presence of cyclic adenosine monophosphate (cAMP) (250 μM) in the cellular incubation medium (the microelectrode solution contained 145 mM N-methylglucamine-Cl). a) Recordings obtained in the two conditions. b) Mean values of P_o in the absence (—○—) or presence (—Δ—) of cAMP (n=4 animals) were related to voltage. c) Single-channel current/voltage (I/V) relationship obtained in the presence of cAMP in the incubation medium (the reversal potential was calculated on the basis of linear regression of points representing outward currents. Values are presented as arithmetic mean±SEM (n=10 animals).

1.9±1.7 mV and -0.5±2.5 mV, respectively (n=7). Both this value and the previous one were not significantly different from 0, or from each other (the mean intercept point was 0.7 mV). The channel presented outwardly-rectifying behaviour: the conductance at positive voltages was 2.4±0.3 pS, and at negative voltages 1.7±0.1 pS (n=7; $p<0.05$). The currents measured at low voltages were not taken into account for the I/V relationship if the corresponding values were less than twice the noise value. The Cl^- channel rundown was at times observed in inside-out recordings (activity fell by 30–50% in the first 5 min). To verify stable channel activity, measurements were prolonged for at least 5 min in control solution.

In the presence of 145 mM N-methylglucamine-Cl inside the microelectrode and of 130 mM N-methylglucamine-gluconate/15 mM N-methylglucamine-Cl on

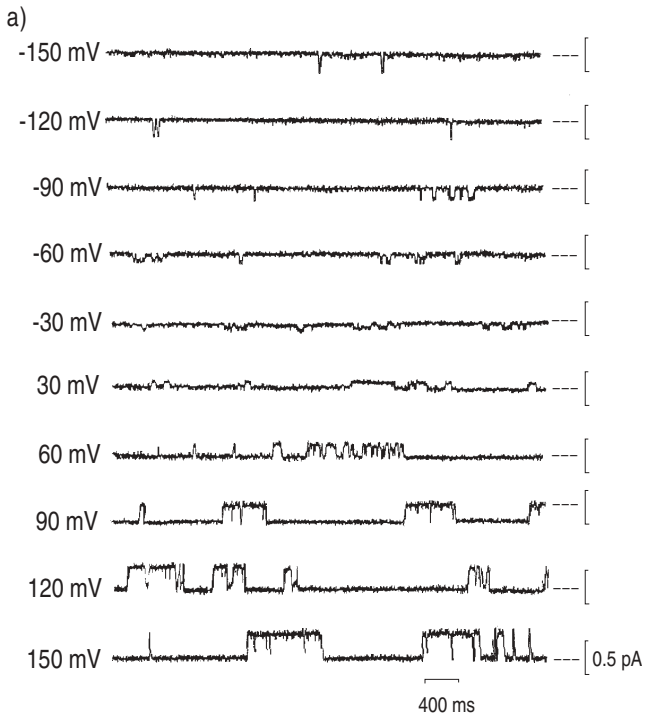

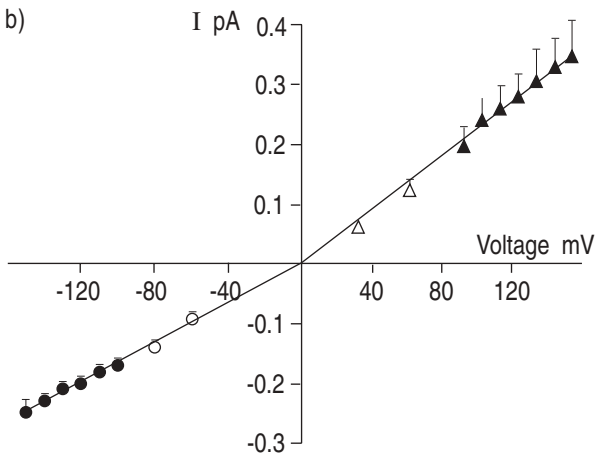

Fig. 3. – Single-channel currents (I) recorded in inside-out configuration in the presence of symmetrical 145 mM N-methylglucamine-Cl. a) Tracings obtained at the voltages indicated. b) Single-channel current/voltage (I/V) relationship. Some amplitudes have been reported as open marks, because they were not used to obtain the I/V relationship (as these amplitudes were less than twice the noise value). Values are presented as arithmetic mean±SEM (n=7 animals).

the cytoplasmic side it was possible to see the presence of channels clearly even at weak positive voltages, in agreement with the behaviour of an anionic channel. A gluconate permeability relative to Cl^- of 0.11 was calculated [23]. After the substitution of N-methylglucamine-Cl with KCl or NaCl on the cytoplasmic side, no changes in current amplitudes were observed and the reversal potential was -0.8 and 0.5 mV, respectively.

In the presence of N-methylglucamine-Cl symmetrical solutions, when the cytoplasmic side free [Ca^{2+}] was increased from 0.2×10^{-7} to 10^{-6} and 10^{-4} M, Po rose without modification in the conductance (Po at 0.2×10^{-7} M free Ca^{2+} was statistically less, at all tested voltages, with respect to values determined at 10^{-6} and 10^{-5} M; $p<0.05$ and $p<0.01$, respectively).

Effects of different inhibitors and of frusemide

In inside-out patches (N-methylglucamine-Cl symmetrical solutions), after pretreating cells with cAMP (250 µM), the addition of NPPB to the cytoplasmic side determined a reduction of Po, which increased in conjunction with the concentration used (at 90 mV the median inhibitory concentration (IC_{50}) was 1.8×10^{-6} M). In the presence of NPPB (10^{-5} M), conductance changed by only a small amount and failed to reach statistical significance (p=0.05–0.01). At 10^{-4} M, a flicker block (*i.e.* rapid fluctuation in current during a channel opening due to interruptions long enough to detect but too brief to resolve as individual events [25]) was noticeable. In cell-attached configuration, after NPPB (10^{-5} M) was added to a cAMP containing incubation medium, the PD_{cm} (whole-cell configuration) depolarized to -21.6± 2.8 mV (n=3). At 70 mV, the Po was reduced by 75% (from 0.24±0.02 to 0.06±0.007 (n=4); $p<0.01$). We observed a decrease in Po of 70–75% even in the presence of NPPB in the microelectrode solution. In inside-out configuration, the effect of DIDS (10^{-5} M, the cytoplasmic side) was a 92% Po inhibition.

We then evaluated the frusemide effects. In inside-out configuration experiments, in the presence of frusemide (from 10^{-5} to 10^{-3} M) on the cytoplasmic side or in the microelectrode solution, no inhibitory effect on Po or on conductance was noted. Conversely, in cell-attached configuration, a cAMP+frusemide solution caused a de-polarization of PD_{cm} (table 1, whole-cell configuration). The PD_{cm} was also evaluated in the presence of 10^{-5} and 10^{-4} M frusemide in the medium using

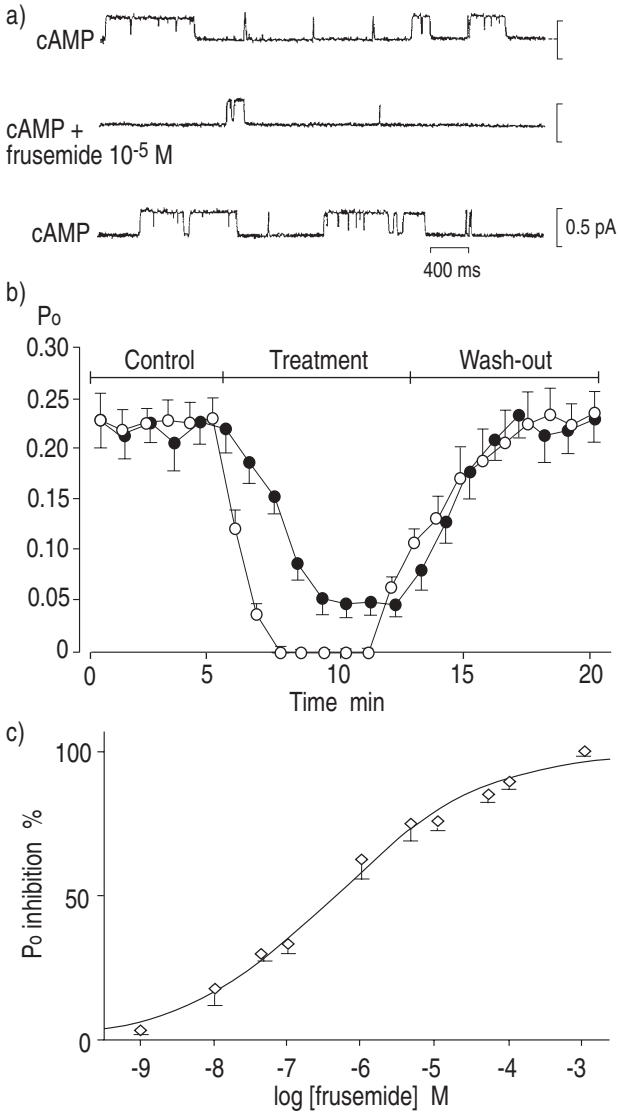

Fig. 4. – Effects of the presence of frusemide in the cellular incubation medium (containing cyclic adenosine monophosphate (cAMP) observed recording Cl^- channel activity in cell-attached configuration and considering a voltage of 70 mV. a) Tracings observed in control conditions, after 4 min of treatment and 6 min after returning to control conditions. b) Time course of the effect of frusemide on open probability (Po) at 10^{-5} M (●; n=5) and at 10^{-3} M (○; n=4), respectively. d) Dose-response curve related to the inhibition of Po due to frusemide. Each point represents the mean percentage of inhibition (±SEM) using experiments from different cell isolations obtained from 4–5 animals.

Table 1. – Cellular membrane electrical potential difference (PD_{cm}) (measured in whole-cell configuration) in the presence of frusemide or bumetanide in the cellular incubation medium (containing cAMP)

	Concentration of drug in incubation medium M										
	10^{-9}	5×10^{-9}	10^{-8}	5×10^{-8}	10^{-7}	10^{-6}	5×10^{-6}	10^{-5}	5×10^{-5}	10^{-4}	10^{-3}
Frusemide											
PD_{cm} mV	-36.6 ±3.1 (n=4)	-	-34.1 ±3.9 (n=4)	-29.6 ±2.6 (n=4)	-28.7* ±2.6 (n=4)	-24.4* ±2.9 (n=4)	-21.7** ±3.1 (n=4)	-21** ±2.4 (n=4)	-19.9** ±3.0 (n=4)	-16.1** ±2.7 (n=4)	-13.6** ±3.1 (n=4)
Bumetanide											
PD_{cm} mV	-34.6 ±3.5 (n=3)	-31.8 ±2.9 (n=4)	-30.6 ±3.3 (n=4)	-	-25.7* ±2.9 (n=4)	-19.9* ±2.4 (n=4)	-	-17.4** ±2.1 (n=4)	-	-14.2** ±2.3 (n=4)	-

Values are presented as mean±SEM. n: number of animals; cAMP: cyclic adenosine monophosphate. *: $p<0.05$; **: $p<0.01$, with respect to the values measured in the absence of the inhibitors, -37.9±2.7 mV (n=6) (see text).

impalements or nystatin perforated-patch technique (the values were -20.6±2.1 mV (n=4) and -18.4±2.6 mV (n=4), respectively, at 10^{-5} M frusemide; and -17.5± 1.7 mV (n=4) and -15.6±2.3 mV (n=4), respectively, at 10^{-4} M frusemide: not significantly different from values determined in whole-cell configuration). At 10^{-5} M, a significant reduction of P_o (fig. 4a) was detected. The time necessary to obtain maximum inhibition was dose-dependent and the effect was reversible (fig. 4a and b). The dose-response curve (obtained at 70 mV) referring to inhibition of P_o presented an IC_{50} of 4.3×10^{-7} M (fig. 4c). No significant effect on conductance was noticed. The presence of 10^{-5} M frusemide in the incubation medium, revealed a,iCl of 12.1±2.2 mM (n=4), a value significantly lower in relation to that observed in the presence of cAMP but not of frusemide ($p<0.05$).

In cell-attached conditions, the effect of frusemide (10^{-5} and 10^{-4} M) present in the incubation medium was also tested on cells not pretreated with cAMP. The PD_{cm} measured with different techniques (whole-cell, impalements) showed no significant variations. The effect on P_o was difficult to detect with respect to the low P_o values observed in the absence of cAMP. At 70 and 110 mV and at the two different frusemide concentrations tested (10^{-5}, 10^{-4} M), the P_o tended to decrease, but not to any significant extent (for instance, at 110 mV the P_o was 0.094± 0.009, and in the presence of 10^{-5} or 10^{-4} M frusemide it was 0.082±0.008 and 0.077±0.007, respectively (n=4)).

In order to obtain indications of the mechanism of frusemide action, cell-attached experiments were also performed using bumetanide. In cell-attached configuration in the presence of bumetanide in the incubation medium, we noted a depolarization of PD_{cm} (table 1), and starting from 10^{-9} to 10^{-4} M a significant decrease in P_o with an $IC_{50}=5.7\times 10^{-8}$ M. In inside-out configuration, the bumetanide, when present on the cytoplasmic side, had no effect.

Discussion

The single-channel conductance evaluated in the present experiments (about 2 pS) presents a value similar to that determined on the basis of noise analysis [3]. The outward rectification, cAMP and $[Ca^{2+}]$ activation and NPPB and DIDS inhibition measured in these single channel recordings are in agreement with the observations in whole-cell experiments [3, 4]. This suggests that the channel that we detected is responsible for current due to Cl^-, revealed in whole-cell experiments.

For some aspects, such as weak voltage dependence, secretagogue activation and NPPB inhibition, this channel is similar to that found in the rat basophilic leukaemia (RBL)-2H3 cell line [5]. However, single-channel conductance is lower (2 *versus* 32 pS), and there is a weak activation by $[Ca^{2+}]$ and an outward rectification not found in cells of the RBL-2H3 line. This confirms the existence in these two kinds of cell of different electrophysiological characteristics already found for cationic channels [24]. The characteristics of the channel examined are, in part, similar to those of some Cl^- channels of other cells [25, 26].

As NPPB is able to act on both sides of an excised patch, its action is certainly directed to the Cl^- channels. The most probable explanation of its effect in cell-attached configuration, when present in the medium, is that it is permeable through the membranes and then acts on the cytoplasmic side of the channel. Analogous effects were observed in similar conditions in RBL cells [5].

The effects of frusemide are different. When it is placed in direct contact with the patch membrane, there is a lack of effect on the Cl^- channel. Conversely, frusemide is able to inhibit when it is present in the incubation medium in cell-attached experiments, suggesting an indirect inhibitory effect. In accordance with this, frusemide is able to act at lower concentrations than usually necessary (10^{-3} M) to inhibit the Cl^- channels [11, 12], and action times are slow. Possible indirect mechanisms of action of frusemide are different.

Frusemide could act on aspecific cationic channels (see rat exocrine pancreas [27]) present in mast cell membrane [2] and, thus, decrease the intracellular $[Ca^{2+}]$ with a consequent decrease in Cl^- channel activity. However, most Ca^{2+} enters the cell through other specific Ca^{2+} channels, the Ca^{2+} sensitivity of Cl^- channels is low and bumetanide is also effective, so this hypothesis seems unlikely.

In any case, frusemide acts on different coupled transport systems, such as Na^+-K^+-$2Cl^-$ [9, 10] Na^+-NH^+_4-$2Cl^-$ [28] symports and Cl^-/HCO_3^- antiport [29]. The inhibition of a Cl^-/HCO_3^- exchange (or of a co-transport Na^+-NH_4^+-$2Cl^-$) can lead to an alteration of intracellular pH and some Cl^- channels are sensitive to pH [30]. However, our preliminary data (not shown) did not reveal, in inside-out configuration, variations of Po with changes of pH on the cytoplasmic side. In reality the most well-known effect of frusemide is on the Na^+-K^+-$2Cl^-$ symport, whose presence on mast cell membrane has recently been suggested [31]. In support of an effect of this kind, there is also the fact that bumetanide (a more specific inhibitor of this symport) is able to inhibit Cl^- channel activity. The IC_{50} of bumetanide is lower than that of frusemide, in agreement with data reported for other cells [10, 32].

Data obtained in whole-cell configuration [4] suggest that, like Cl^- channels of myocytes [26], the activity of the channels in question would decrease with the fall in intracellular free sodium $[Na^+]$. The blocking of a Na^+-K^+-$2Cl^-$ symport may lead to a decrease in the Cl^- channel activity with this procedure. The lack of inhibitory effect of frusemide in the absence of cAMP might lead one to suppose that the possible action of the decrease of intracellular $[Na^+]$ is exercised on the Cl^- channel activity by means of interaction with the cAMP dependant mechanism of the Cl^- channel activation [4].

The decrease in Cl^- channel activity, as a consequence of the blocking of a Na^+-K^+-$2Cl^-$ symport, might also be due merely to the decrease in intracellular free chloride $[Cl^-]$. However, in whole-cell configuration, variations of intracellular $[Cl^-]$ from 34 to 11 mM had no detectable effect on the cAMP activation [4] of Cl^- currents. In addition, our preliminary data (not shown) indicated that, in inside-out configuration, reducing the $[Cl^-]$ in the cytoplasmic side solution caused no significant variations in the P_o.

Against the hypothesis of the existence of a Na^+-K^+-$2Cl^-$ co-transport is the observation that, *in vivo*, there is no protective action of bumetanide against bronchial asthma caused by airway challenges that probably act

through the release of mast cell mediators [6]. However, it should be noted that frusemide acts as an antiasthma medication only when inhaled and not when taken orally. *In vivo* inhaled bumetanide offers no protection against bronchial asthma, despite the fact that *in vitro* studies have shown an inhibitory effect of bumetanide against neurally-induced airway smooth muscle contraction that is 10 times stronger than for frusemide [33]. This suggests that distribution, metabolism and clearance of the inhaled diuretics at the level of the airway submucosa is not clear, and may be different for each loop diuretic.

References

1. McFadden ER Jr. Asthma: morphologic-physiologic interactions. *Am J Respir Crit Care* 1994; 150: 523–526.
2. Matthew G, Neher E, Penner R. Second messenger-activated calcium influx in rat peritoneal mast cells. *J Physiol (Lond)* 1989; 418: 105–130.
3. Matthew G, Neher E, Penner R. Chloride conductance activated by external agonist and internal messengers in rat peritoneal mast cells. *J Physiol (Lond)* 1989; 418: 131–144.
4. Dietrich J, Lindau M. Chloride channels in mast cells: block by DIDS and role in exocytosis. *J Gen Physiol* 1994; 104: 1099–1111.
5. Romanin C, Reinsprecht M, Pecht I, Schindler H. Immunologically activated chloride channels involved in degranulation of rat mast cells. *EMBO J* 1991; 10: 3603–3608.
6. Chung KF, Barnes PJ. Loop diuretics and asthma. *Pulm Pharmacol* 1992; 5: 1–7.
7. Rodwell LT, Anderson SD, du Toit J, Seale JP. Different effects of inhaled amiloride and furosemide on airway responsiveness to dry air challenge in asthmatic subjects. *Eur Respir J* 1993; 6: 855–861.
8. Berti F, Rossoni G, Zuccari G, *et al.* Protective activity of inhaled furosemide against immunological respiratory changes and mediator release in guinea-pigs. *Pulm Pharmacol* 1992; 5: 115–120
9. Palfrey HC, Feit PW, Greengard P. cAMP stimulated cation co-transport in avian erythrocytes: inhibition by "loop" diuretics. *Am J Physiol* 1980; 238: C139–C148.
10. Schlatter E, Greger R, Weidtke C. Effect of "high ceiling" diuretics on active salt transport in the cortical thick ascending limb of Henle's loop of rabbit kidney: correlation of chemical structure and inhibitory potency. *Pflügers Arch* 1983; 396: 210–217.
11. Patarca R. Candia OA, Reinach PS. Mode of inhibition of active chloride transport in the frog cornea by furosemide. *Am J Physiol* 1983; 245: F660–F669.
12. Evans MG, Marty A, Tan YP, Trautman A. Blockage of Ca-activated Cl^- conductance by furosemide in rat lacrimal glands. *Pflügers Arch* 1986; 406: 65–68.
13. Penner R, Pusch M, Neher E. Wash-out phenomena in dialyzed mast cells allow discrimination of different steps in stimulus-secretion coupling. *Bioscience Rep* 1993; 7: 313–321.
14. Spicer SS. Histochemical properties of mucopolysaccharide and basic protein in mast cell. *Ann NY Acad Sci* 1963; 103: 322–332.
15. Fabiato A, Fabiato F. Calculator programs for computing the composition of the solution containing multiple metals and ligands used for experiments in skinned muscle cells. *J Physiol (Paris)* 1979; 75: 463–505.
16. Fabiato A. Time and calcium dependence of activation and inactivation of calcium-induced release of calcium from sarcoplasmic reticulum of a skinned canine Purkinje's cell. *J Gen Physiol* 1985; 85: 247–289.
17. Meyer G. Large-conductance K^+ channels and their regulation in epithelial cells of guinea-pig gall-bladder. *Bioelectrochem Bioenerg* 1995; 36: 23–31.
18. Hamill CR, Mary A, Neher E, Sakmann B, Sigworth FJ. Improved patch-clamp technique or high resolution current recording from cells and cell free membrane patches. *Pflügers Arch* 1981; 391: 85–100.
19. Copello J, Heming Y, Segal Y, Reuss L. cAMP-activated apical membrane chloride channels in Necturus gall-bladder epithelium. *J Gen Physiol* 1993; 102: 177–199.
20. Korn S, Korn R. Influence of sodium-calcium exchange on calcium current run down and the duration of calcium-dependent chloride currents in pituitary cells studied with whole cell and perforated patch recording. *J Gen Physiol* 1989; 94: 789–812.
21. Henin S, Cremaschi D. Transcellular ion route in rabbit gall-bladder. *Pflügers Arch* 1975; 355: 125–139.
22. Cremaschi D, James PS, Meyer G, Rossetti C, Smith MW. Developmental changes in intraenterocyte cation activities in hamster terminal ileum. *J Physiol* 1984; 354: 363–373.
23. Meyer G, Henin S, Cremaschi D. Cell K^+ activity in the rabbit gall-bladder. *Bioelectrochem Bioenerg* 1981; 8: 575–579.
24. Edelman A, Curci S, Samarzija I, Fromter E. Determination of intracellular K^+ activity in rat kidney proximal tubular cells. *Plfügers Arch* 1978; 378: 37–45.
25. Yellen C. Ionic permeation and blockade in Ca^{2+}-actuated K^+ channels of bovine chromaffin cells. *J Gen Physiol* 1984; 84: 157–186.
26. Lindau M, Fernandez JM. A patch-clamp study of histamine-secreting cells. *J Gen Physiol* 1986; 88: 349–368.
27. Marty A, Tan YP, Trautman A. Three types of calcium dependent channel in rat lacrimal glands. *J Physiol (Lond)* 1984; 357: 293–325.
28. Bahinsky A, Nairn AC, Greengard P, Gadsby DC. Chloride conductance regulated by cyclic AMP-dependent protein kinase in cardiac myocytes. *Nature* 1989; 340: 718–721.
29. Goghelein H. Chloride channels in epithelia. *Biochim Biophys Acta* 1988; 947: 521–547.
30. Watts BA, Good DW. Effects of ammonium on intracellular pH in rat medullary thick ascending limb: mechanism of apical membrane NH_4^+ transport. *J Gen Physiol* 1994; 103: 917–936.
31. Aronson PS. Ion transport processes in apical membranes of epithelia. *Fed Proc* 1984; 43: 2473–2487.
32. Park K, Brown PD. Intracellular pH modulates the activity of chloride channels in isolated lacrimal gland acinar cells. *Am J Physiol (Cell Physiology)* 1995; 37(3): C647–C650.
33. Friis UG, Johansen T, Hayes NA, Foreman JC. IgE-receptor activated chloride uptakes in relation to histamine secretion from rat mast cells. *Br J Pharmacol* 1994; 111: 1179–1183.
34. Haas M. Properties and diversity of (Na-K-Cl) co-transporters. *Ann Rev Physiol* 1989; 51: 443–457.
35. Elwood W, Lotwall JO, Barnes PJ, Chung KF. Loop diuretics inhibit cholinergic and non-cholinergic nerves in guinea-pig airways. *Am Rev Respir Dis* 1991; 143: 1340–1344.